Journal of Cerebral Blood Flow and Metabolism
16:1236–1249 © 1996 The International Society of Cerebral Blood Flow and Metabolism
Published by Lippincott–Raven Publishers, Philadelphia

Reduced Transit-Time Sensitivity in Noninvasive Magnetic Resonance Imaging of Human Cerebral Blood Flow

*D. C. Alsop and *†J. A. Detre

*Departments of *Radiology and †Neurology, University of Pennsylvania Medical Center, Philadelphia, Pennsylvania, U.S.A.*

Summary: Herein, we present a theoretical framework and experimental methods to more accurately account for transit effects in quantitative human perfusion imaging using endogenous magnetic resonance imaging (MRI) contrast. The theoretical transit time sensitivities of both continuous and pulsed inversion spin tagging experiments are demonstrated. We propose introducing a delay following continuous labeling, and demonstrate theoretically that introduction of a delay dramatically reduces the transit time sensitivity of perfusion imaging. The effects of magnetization transfer saturation on this modified continuous labeling experiment are also derived, and the assumption that the perfusion signal resides entirely within tissue rather than the arterial microvasculature is examined. We present results demonstrating the implementation of the continuous tagging experiment with delay on an echoplanar scanner for measuring cerebral blood flow (CBF) in normal volunteers. By varying the delay, we estimate transit times in the arterial system, values that are necessary for assessing the accuracy of our quantification. The effect of uncertainties in the transit time from the tagging plane to the arterial microvasculature and the transit time to the tissue itself on the accuracy of perfusion quantification is discussed and found to be small in gray matter but still potentially significant in white matter. A novel method for measuring T_1, which is fast, insensitive to contamination by cerebrospinal fluid, and compatible with the application of magnetization transfer saturation, is also presented. The methods are combined to produce quantitative maps of resting and hypercarbic CBF. **Key Words:** Magnetic resonance imaging—Arterial transit time—Perfusion—Functional imaging.

Since magnetic resonance imaging (MRI) scanners are widespread in both clinical and research environments, the availability of a quantitative MRI perfusion imaging technique would help to increase the use of perfusion imaging as a diagnostic tool. Additionally, MRI methods do not require a radioactive tracer, are directly superimposable onto high resolution anatomic images acquired within the same imaging session, and can potentially achieve spatial resolution that is orders of magnitude better than that of radionuclide methods. MRI methods based on the injection of a magnetic contrast agent have yielded excellent images of cerebral blood volume (CBV) (Belliveau et al., 1990), but quantification of perfusion with these methods is more challenging (Weisskoff et al., 1993). The need for bolus injection of a contrast agent also dramatically reduces the number of repeated measures possible within a single examination and decreases the advantage of MRI over positron emission tomography (PET) flow techniques.

MRI measurements of perfusion may also be obtained using an endogenous tracer. In this approach, arterial water is tagged proximal to the brain using spatially selective excitation or inversion pulses. Effects of arterial tagging on distal images can be quantified in terms of tissue perfusion since the regional changes in signal intensity are determined by blood flow and T_1 relaxation. Several types of tagging strategies have been employed. Repeated saturation (Detre et al., 1992) and continuous adiabatic inversion (Dixon et al., 1986, Williams et al., 1992) both approximate a continuous tagging of blood as it flows across a plane located proximal to the slice location. Using the adiabatic inversion technique, alterations of blood flow due to modulation of blood P_aCO_2 (Williams et al., 1992), seizures (Williams et al., 1993), cold injuries (Williams et al., 1992), and amphetamine stimulation (Silva et al., 1995) in rats have been reliably quantified. The alternative to these continuous labeling techniques is single-pulse tagging of an extended slab of tissue containing a sizable volume of arterial blood

Received October 6, 1995; final revision received May 3, 1996; accepted May 15, 1996.

Address correspondence and reprint requests to Dr. David C. Alsop at Department of Radiology, University of Pennsylvania Medical Center, 3400 Spruce Street, Philadelphia, PA 19104, U.S.A.

Abbreviations used: CBF, cerebral blood flow; CSF, cerebrospinal fluid; FOV, field of view; MR, magnetic resonance; MRI, magnetic resonance imaging; RF, radiofrequency; TE, spin echotime; TR, repetition time.

(Edelman et al., 1994, Kwong et al., 1995); current methods for quantifying single-pulse experiments are less well developed (see below).

Implementation of the above perfusion imaging strategies for human studies presents several challenges. Humans are typically studied at field strengths lower than those used for small animals, thus resulting in lower signal-to-noise ratios and shorter T_1 relaxation times. Transit times from proximal arteries are also longer in humans. Long transit times greatly reduce the sensitivity of the perfusion measurement. Since longer transit times affect the observed signal intensity, uncertainty in the transit time will also result in inaccuracies in flow quantification. Another problem, always present in human studies, is subject motion and associated artifacts. Because perfusion imaging must detect small percentage changes in an image, motion effects can easily degrade the perfusion images. Rigid fixation of the head and paralytic agents, both of which are frequently used in animal perfusion studies, cannot be used to prevent motion of human subjects without substantial discomfort.

Several groups have made first steps towards quantitative perfusion imaging in humans, but the problems outlined above have not all been addressed. One group (Roberts et al., 1994) reported human perfusion images employing an adaptation of the adiabatic inversion technique to fast gradient echo imaging. Although quantitative perfusion values in agreement with literature values were obtained, the imaging technique was highly sensitive to the arterial transit time assumed and did not suppress or account for the large contribution of intraluminal spins. A second group (Edelman et al., 1994) reported a slab inversion technique that highlights the effects of transit time in the human arterial tree by tagging a bolus of blood whose transit through the arterial system is observed in images obtained at different delays between inversion and image acquisition. Their method incorporated echoplanar imaging to reduce motion by obtaining tagged and control images spaced only a few seconds apart. The signal intensity in this method can be highly dependent on transit time. Fitting of multiple images acquired with different delays has been suggested as a route towards quantification (Buxton et al., 1995), but assumptions about the distribution of velocities and transit times in the tagged arteries are required. An alternative spatial inversion tagging scheme, based on a method developed earlier for detecting brain activation (Kwong et al., 1992) has been proposed, (Kwong et al., 1995). This tagging method has also been used for mapping brain activation (Kim, 1995). The flow-dependent signal change is identical to that of the other pulsed method (Edelman et al., 1994).

Herein, we present a theoretical framework and experimental methods to more accurately account for transit effects in quantitative human perfusion imaging. We begin by deriving the transit time sensitivity of both the continuous and pulsed inversion spin tagging experiments and demonstrating that by introducing a delay following continuous labeling, transit effects are markedly reduced without sacrificing sensitivity. The continuous tagging experiment is then implemented on an echoplanar scanner and used for imaging of normal volunteers. By varying the delay, we estimate transit times in the arterial system, values that are necessary for assessing the accuracy of our quantification. A novel method for measuring T_1 that is fast and insensitive to contamination by cerebrospinal fluid (CSF) is also presented. Finally, the methods are combined to produce quantitative maps of resting and hypercarbic CBF.

THEORY

Continuous labeling experiments

The signal intensity change observed in the continuous labeling experiment, as illustrated in figure 1a, was derived previously (Williams et al., 1992).

$$M_b^{tag} - M_b^{ctrl} = -T_{1app} \exp\left(\frac{-\delta}{T_{1a}}\right) 2\alpha \frac{fM_b^0}{\lambda} \qquad (1)$$

where f is the blood flow in $ml/g^{-1}\ s^{-1}$; λ is the brain–blood partition coefficient (defined as ml of water per gram tissue / ml water per ml blood); δ is the arterial transit time from the tagging plane to the imaged slice; T_{1b} is the T_1 of brain tissue; T_{1a} is the T_1 of arterial blood; α is the inversion efficiency (Williams et al., 1992), which should be one for perfect inversion and 0.5 for perfect saturation; M_b^{tag} is the brain tissue magnetization in the tagged experiment; M_b^{ctrl} is the brain tissue magnetization in the control experiment; M_b^0 is the equilibrium brain tissue magnetization; and T_{1app} is given by

$$\frac{1}{T_{1app}} = \frac{1}{T_{1b}} + \frac{f}{\lambda} \qquad (2)$$

Notice that the observed signal is exponentially dependent on the arterial transit time, δ. In the rat experiments, the short transit times of the cerebral vasculature and the long T_1 of blood at the high (4.7 Tesla) field strength reduced the importance of transit time measurement (Williams et al., 1993). For human perfusion, however, transit time dependence of the measured CBF is significant and represents a major obstacle to accurate quantification. Measurement of vascular transit time to accompany each perfusion measurement would reduce the sensitivity and temporal resolution of the method.

One approach to reducing the transit time sensitivity of continuous spin labeling experiments is to introduce a delay of duration, w, between the end of tagging and image acquisition (Fig. 1**B**). If w is less than δ, the delay

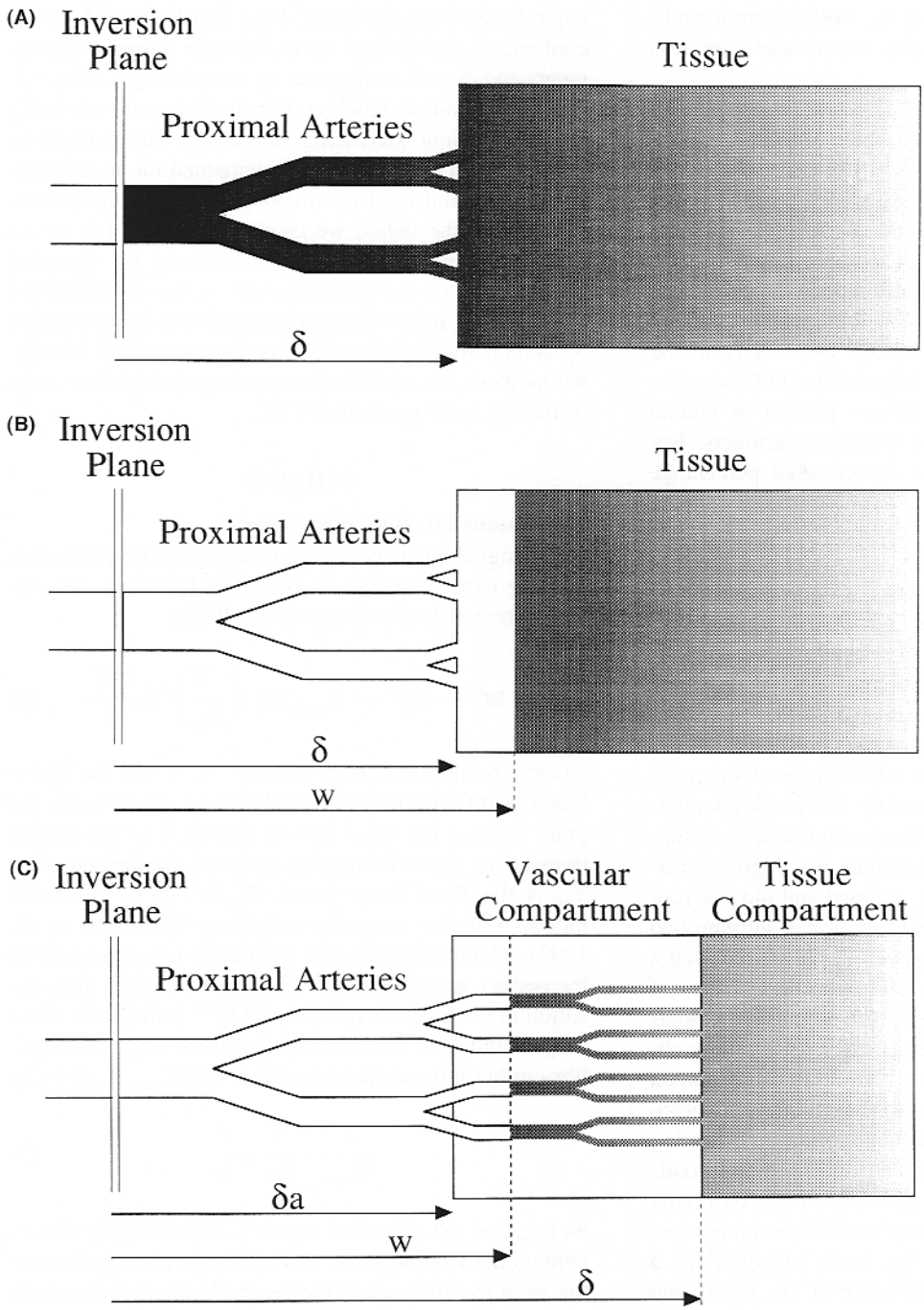

FIG. 1. Schematic diagrams of the continuous arterial tagging perfusion imaging models. **A:** In previous implementations, arterial spins are inverted as they pass the inversion plane. Tagged spins gradually relax back towards equilibrium as they diffuse into the tissue. δ is defined as the transit time from the inversion plane to the tissue. **B:** When a delay of duration, w, is introduced, the proximal artery signal is eliminated, and uninverted spins may enter the tissues before imaging. If δ increases, fewer uninverted spins arrive in the tissue resulting in an increase in signal. This increase largely cancels the loss of signal resulting from increased T_1 decay of tagged spins before they arrive in the tissue. **C:** In a more complex model, the contribution of intraluminal spins is explicitly accounted for by separating the "tissue" seen in **(a)** and **(b)** into a vascular compartment and a true tissue compartment. A second transit time, δa, from the inversion plane to the arterial vascular compartment, is defined.

has no effect but if w is longer than δ, the signal is given by (see Appendix)

$$M_b^{tag} - M_b^{ctrl} = -T_{1app}\exp\left(\frac{-w}{T_{1app}}\right) \exp\left(-\delta\left[\frac{1}{T_{1a}} - \frac{1}{T_{1app}}\right]\right) 2\alpha \frac{fM_b^0}{\lambda} \quad (3)$$

Notice that the flow now depends on δ times the difference between the tissue and arterial blood relaxation rates. Fortunately, the T_1 in gray matter and arterial blood are within 10% of each other at 1.5 Tesla, so the transit time sensitivity of the expression is markedly reduced. For white matter, which has a shorter T_1, the delay is only partially effective at reducing transit time sensitivity.

In the above theory, we have ignored the effects of magnetization transfer on image intensity. This is correct if a separate tagging radiofrequency coil is used (Silva et al., 1995), since power deposition at the imaging slice is

minimal. In the present study, a single coil was used for both tagging and imaging, so magnetization transfer effects are significant. Magnetization transfer can alter the observed signal in two ways (Zhang et al., 1992). First, application of the tagging pulse causes a decreased signal from the imaged slice even in the absence of perfusion. We will assume that the control experiment also experiences this attenuation so that subtraction of the two images is predominantly dependent on perfusion. The presence of the off-resonance saturation also causes a decrease in the T_{1app}. Although theoretical expressions for saturated T_{1app} have been reported (Zhang et al., 1992), we choose to assume only that the decay during the application of a tagging pulse is characterized by a single T_{1app}, T_{1s} which may be different from T_{1ns}, T_{1app} in the absence of off-resonance radiofrequency (RF) saturation (Yeung and Swanson, 1992). If magnetization transfer saturation is present, the solution becomes (see Appendix)

$$M_b^{tag} - M_b^{ctrl} = \frac{-2\,M_b^0\,f\alpha T_{1ns}}{\lambda}\exp(-\delta/T_{1a})\left[\exp(\min(\delta - w,0)/T_{1ns}) - \exp(-w/T_{1ns})\left(1 - \frac{T_{1s}}{T_{1ns}}\right)\right] \quad (4)$$

where the min ( ) function returns the smaller of its two arguments.

Pulsed tagging experiments

The signal change in the pulsed tagging experiments depends primarily on the geometry of the tagged slab. The signal is given by (see Appendix)

$$M_b^{tag} - M_b^{ctrl} = -\exp\left(\frac{-TI}{T_{1app}}\right) 2\alpha \frac{fM_b^0}{\lambda} \frac{\left[\exp\left(\min(TI, \delta + \tau)\left(\frac{1}{T_{1app}} - \frac{1}{T_{1a}}\right)\right) - \exp\left(\delta\left(\frac{1}{T_{1app}} - \frac{1}{T_{1a}}\right)\right)\right]}{\left(\frac{1}{T_{1app}} - \frac{1}{T_{1a}}\right)} \quad (5)$$

where TI is the time between tagging and imaging, δ is now the transit time from the most distal portion of the slab to the tissue, and τ represents the duration of the bolus. If TI is greater than $\delta + \tau$, then absolute perfusion quantification is problematic, (see Appendix). If TI is less than $\delta + b$, and T_{1app} is comparable to T_{1a}, the expression can be approximated as

$$M_b^{tag} - M_b^{ctrl} = -\exp\left(\frac{-TI}{T_{1app}}\right) 2\alpha \frac{fM_b^0}{\lambda}(TI - \delta) \quad (6)$$

TI must be large compared to δ in order to achieve insensitivity to transit time. Since the signal intensity decays with T1, increasing TI to much greater than δ wiill significantly reduce the sensitivity of the measurement.

Comparison of tagging techniques

In Fig. 2, we compare the signal intensity observed with the two tagging techniques. Figure 2**A** shows the theoretical signal intensities in gray matter for a flow of 60 ml 100 g^{-1} min^{-1} assuming a T_{1app} of 1,000 ms (Larsson et al., 1988; Steen et al., 1994), and T_{1a} of 1,100 ms (Bryant et al., 1990). The continuous inversion experiment with no delay gives the highest signal intensity of all the techniques. As the delay, w, is increased, the maximum signal intensity decreases but the signal becomes very insensitive to the transit time for transit times shorter than w. The signal in the pulsed inversion experiment is smaller and more sensitive to transit time than the continuous inversion experiment with a delay. Figure 2**B** shows the signal intensities calculated for white matter. Because the T_1 of white matter, 600 ms, is considerably smaller than that of blood, the signal from continuous labeling experiments increases with transit time. The pulsed inversion experiments retain their sensitivity to transit times.

Figure 2 suggests that continuous inversion is superior to pulsed inversion, but other factors may influence the success of the experiment. If only a single slice is being imaged, the transit time can be reduced slightly in pulsed inversion experiments by moving the inverted slab closer to the slice. Nevertheless, continuous labeling with a delay appears to be an attractive perfusion imaging strategy and we have pursued it exclusively in the remainder of this study.

Contribution of intraluminal spins

Intraluminal spins have been ignored in the past, partly because bipolar gradients were applied to attenuate the signal from flowing spins (Williams et al., 1992). Recent theoretical calculations (Henkelman et al., 1994) have demonstrated, however, that a substantial fraction of the blood signal is not attenuated by these gradients. This has several implications for perfusion imaging. First, it is nearly impossible to accurately measure the transit time to the tissue, δ, with magnetic resonance (MR) since it is difficult to discriminate spins in the tissue from spins in the microvasculature. Second, if the arterial blood volume is large enough, the signal from blood may dominate the signal from the tissue. This is especially true in white matter where short T_{1app} reduces the observed perfusion signal from tissue. In order to assess the contribution of these two uncertainties to the quantification of perfusion, we expanded our model to include an arterial vasculature compartment. We divide the signal from the image into a brain tissue compartment and a vascular compartment. The signal from the tissue compartment

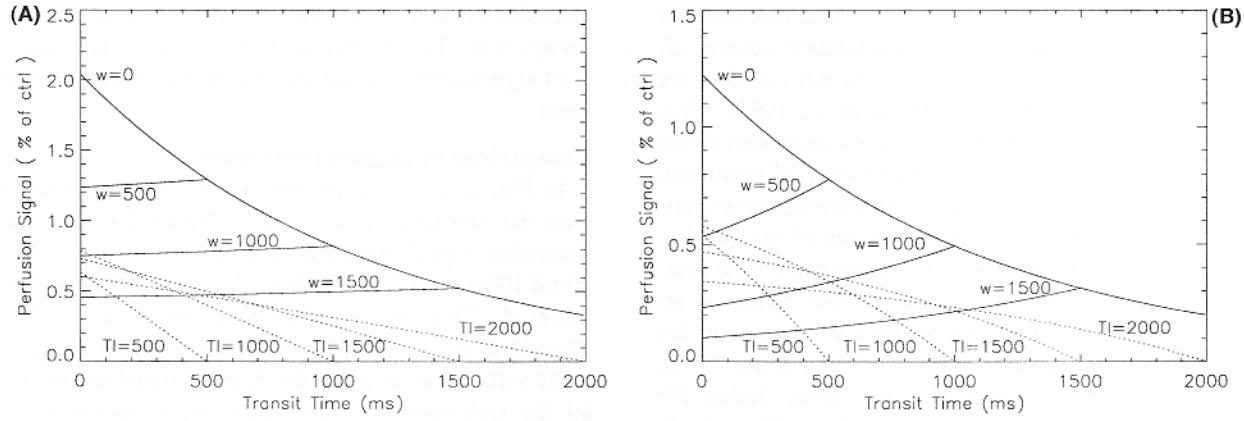

FIG. 2. Theoretical image signal intensity for a flow of 60 ml 100 g^{-1} min^{-1} as a function of tissue transit time calculated for both continuous and pulsed inversion experiments in gray matter **(A)** and white matter **(B)** using Eqs. 3 and 5. Calculated signals for continuous tagging with delays of 0, 500, 1,000, and 1,500 ms are shown with solid lines. Results for pulsed inversion experiments using TIs of 500, 100, 1,500, and 2,000 ms are plotted with dotted lines. Pulsed inversion experiments assume that τ is longer than TI. Gray matter signal intensity is virtually independent of transit time when continuous tagging with a delay is used, but decays exponentially in the absence of the delay. White matter signal using continuous tagging with a delay increases slightly with transit time, but is still less sensitive than when no delay is employed.

was calculated above. We define a second transit time, δa, which represents the time required for blood to flow from the tagging slice to the arteries within the vascular compartment, illustrated in Fig. 1**C.** The division between the vascular compartment and larger feeding arteries located within the slice is somewhat arbitrary. If bipolar gradients are applied, some estimate of the minimum size of vessels experiencing attenuation is required. Otherwise, the division can be defined by the requirement that the length of blood vessels within the vascular compartment should not exceed the size of a voxel so that spatial resolution is not compromised. The signal from the vascular compartment is given by

$$M_v^{tag} - M_v^{ctrl} = \frac{-2\,M_b^0\,f\alpha T_{1a}}{\lambda}\,[\exp\,((\min(\delta a - w,0) - \delta a)(/T_{1a}) - \exp((\min(\delta - w,0) - \delta)/T_{1a})] \quad (7)$$

where M_v represents the magnetization in the vascular compartment. Notice that for δa less than w, δa completely disappears from the equation and the signal is perfectly independent of arterial transit time. Since the division between the vascular compartment and the feeding vessels is vague, this independence is fortunate. By defining δa, f, and δ, we have implicitly defined the volume of the vascular compartment, V_a, because it is given by

$$V_a = f(\delta - \delta a) \quad (8)$$

It is this relationship that implicitly determines the relative weighting given to the signals from the vascular and tissue compartments.

Some other effects of the intraluminal spins were neglected because they were presumed small. First, we neglected the contribution of the vascular compartment spins to the equilibrium tissue magnetization, M_b^0, because the arterial blood volume should be less than a few percent. We have also ignored magnetization transfer effects within the arterial blood because they are much smaller than those in tissue (Morrison and Henkelman, 1995).

Calculation of flow

To obtain quantitative images of CBF, the above expressions must be inverted, i.e.,

$$f = \frac{-\lambda(M^{tag} - M^{ctrl})}{2\alpha M_b^0}\,C(T_{1ns}, T_{1s}, T_{1a}, \delta, \delta a) \quad (9)$$

where

$$\frac{1}{C} = T_{1ns}\exp(-\delta/T_{1a})\left[\exp(\min(\delta - w,0)/T_{1ns}) - \exp(-w/T_{1ns})\left(1 - \frac{T_{1s}}{T_{1ns}}\right)\right] + T_{1a}[\exp((\min(\delta a - w,0) - \delta a)/T_{1a}) - \exp((\min(\delta - w,0) - \delta)/T_{1a})]$$

METHODS

All imaging was performed in a GE SIGNA 1.5 T scanner (General Electric, Milwaukee, WI, U.S.A.) equipped with a prototype three-axis whole body gradient system capable of echoplanar imaging. Subjects lay prone on the scanner table with their heads within the commercial quadrature RF head

coil. Sagittal T_1-weighted images were obtained prior to selection of an axial slice near the top of the thalamus. This slice was chosen since it included a diversity of tissue types, including white matter, ventricles, cortical gray matter, and deep nuclei. Gradient echo echoplanar images were acquired with a FOV of 24 cm, a flip angle of 90°, a 5-mm slice thickness, an effective spin echo-time (TE) of 31 ms, and a 64 × 64 matrix. Prior to the echoplanar acquisition, fat saturation and perfusion tagging were applied.

Adiabatic inversion was performed following the theory described in Williams et al. (1992). A constant axial gradient of 0.25 G/cm was applied simultaneously with constant RF of 35 mG amplitude. The frequency offset was set at 4,000 Hz resulting in an inversion plane 4 cm from the slice location, approximately midpons. At this level, both carotid and vertebral arteries are oriented in a superior-inferior direction. Echoplanar images were acquired with a repetition time of 4s. The inversion RF and gradient were applied constantly between the image acquisitions except for a variable delay between the end of the tagging and the acquisition of the image. The sign of the frequency offset was alternated to acquire both a proximal inversion image and distal inversion image, the latter of which is used as the unlabeled control. In addition, alternate pairs of proximal and distal inversion images were acquired with tagging gradients of opposite sign in some of the subjects. Changing both the frequency of the RF and the sign of the gradient has been suggested to reduce imperfections in the subtraction of the tagged and control images (Pekar et al., 1996). From 15 to 30 pairs of images were acquired and magnitude averaged for each delay and frequency offset.

Seven normal volunteers, five men and two women, 20–40 years of age were studied. In four of the subjects, images were obtained with posttagging delays of 10, 75, 150, 300, 450, 600, 900, and 1,200 ms. These images were used to assess the vascular transit times. Five of the subjects were imaged with the alternating gradient strategy at a fixed delay of 900 ms. Two of the subjects for this second experiment also participated in the transit time study. T_1 maps were obtained in these five subjects, as described below. In two of these subjects, an additional perfusion image was acquired during mild hypercapnia produced by voluntary hypoventilation.

To quantify the perfusion images, T_{1s} and T_{1ns} were measured by applying off-resonance RF pulses while the perfusion gradient was turned off. The off-resonance pulses caused changes in the signal amplitude due to magnetization transfer. A repetition time (TR) of 8 s was used to assure an equilibrium condition existed prior to RF pulse changes. T_{1s} was measured by obtaining images with 0 delay while the tagging pulse was set to each of 0, 50, 100, 200, 300, 500, 800, 1,000, and 3,500 ms durations. T_{1ns} was measured by applying a long tagging pulse with delays before imaging spanning the same range of durations. The resulting signal decay curves were fit to exponential functions using a nonlinear least squares algorithm. Pixels in which the signal did not change more than 10% when the tagging pulse was applied were assumed to be primarily CSF, which is not attenuated by magnetization transfer, and T_1 was not calculated. Although this method of T_1 measurement is not standard, it is fast, compatible with applied saturation pulses during relaxation, and free from contamination by CSF, which has a much longer T_1 than does gray or white matter.

Quantitative perfusion images were calculated using the formula presented in the previous section, the T_1 maps, and assumptions for the vascular transit times which will be described below. Images were segregated into gray and white matter regions based on T_1, and the gray matter was then manually subdivided into cortical and subcortical regions. Subcortical gray matter included regions of caudate, putamen, and thalamus. Quantitative flows were calculated in each of the five subjects.

RESULTS

A representative set of difference images (control – arterial spin tagging) are displayed in Fig. 3. The first image, obtained with a tagging delay time of only 10 ms, shows a strong perfusion-related signal, but the spatial distribution deviates from the expected cortical gray matter distribution. Except for the ventricles, which are totally dark, both gray and white matter are bright. Extremely bright foci, probably representing large vessels, are readily apparent and account for a considerable part of the total intensity in the image. As the tagging delay is increased, the entire image begins to fade, but the vascular signal decays much more rapidly than does the tissue signal. At delay times of $\geqslant$600 ms, the perfusion image takes on an intensity distribution that follows the cortical structure. Elevated flow relative to white matter is also apparent in the deep nuclei. The bright diagonal linear structures at the medial borders of the thalamus likely represent choroid plexus.

Approximate transit times can be inferred from the properties of the signal as a function of tagging delay. As can be seen in Fig. 3, large arterial structures completely disappear only when a 600 ms delay is used. Figure 4 shows this signal decay with delay in several types of regions averaged over four subjects. The signal from the first region, large arterial structures, begins to decay rapidly with delay except for an initial plateau at the earliest delays indicating an average transit time to these vessels on the order of 200 ms. The signals from these arterial structures, all within gray matter, only decrease to the level of other gray matter regions at ~600 ms delay. Signal from large gray matter regions, including some bright signal regions that probably represent smaller arterial structures, show a longer initial plateau indicating an average transit time of ~400 ms. Finally, gray matter regions selected for the absence of bright structures show very little change with delay. These values of transit times can be used to help constrain the transit times of the model, δa, and δ. δa can readily be constrained to <600 ms based on these results. δ must be >600 ms, but the upper limit is not well constrained by our observations.

T_{1ns} and T_{1s} were successfully measured for both gray matter and white matter. Representative T_{1ns} and T_{1s} images are shown in Fig. 5. T_{1ns} is noticeably $>T_{1s}$ in both gray and white matter regions. T_{1s} was 746 ± 18 ms in gray matter and 525 ± 36 ms in white matter averaged across five subjects. T_{1ns} was longer in both cases, 1151 ± 12 ms for gray matter and 770 ± 11 ms for white matter, in reasonable agreement with other measure-

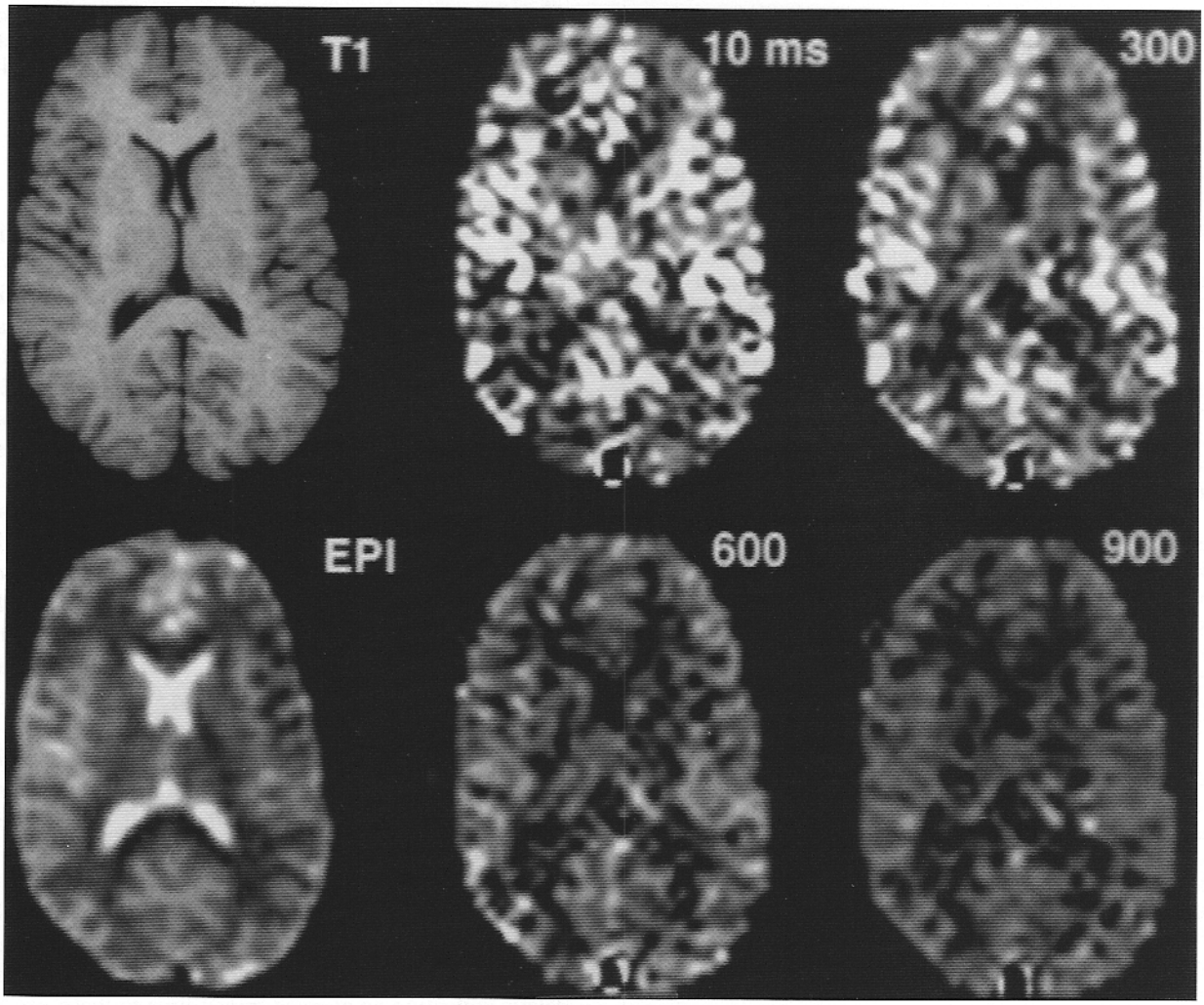

FIG. 3. Difference images (control – arterial spin tagging) acquired with post tagging delays from 10 to 900 ms. A high resolution T_1-weighted image (top left) and an echoplanar image (bottom left) are shown to demonstrate the anatomy. Bright intravascular spins are apparent when short delays are used, but longer delay images show primarily gray and white matter contrast consistent with lower white matter perfusion.

ments of T_1 at 1.5T (Bottomley et al., 1984; Larsson et al., 1988; Steen et al., 1994).

In five of the subjects, the sign of both the frequency and the gradient were alternated in a four-step cycle (Pekar et al., 1996). When the images with opposite gradient sign were averaged separately, the two resulting perfusion-weighted images sometimes differed in intensity. Subtraction of the two perfusion images yielded an error

TABLE 1. *Quantitative perfusion values obtained during rest (n = 5) and during voluntary hypoventilation (n = 2).*

				Gray matter CBF				
Subject	Condition	Age	Sex	Cortical (ml 100 g^{-1} min^{-1})	Subcortical (ml 100 g^{-1} min^{-1})	Total (ml 100 g^{-1} min^{-1})	White matter CBF (ml 100 g^{-1} min^{-1})	Total CBF (ml 100 g^{-1} min^{-1})
1	Resting	23	F	104.3	97.9	103.3	38.3	84.6
2	Resting	25	F	109.9	97.1	107.5	51.2	88.5
3	Resting	25	M	83.0	70.7	80.8	35.4	63.6
4	Resting	31	M	81.8	79.9	81.6	29.5	60.9
5	Resting	35	M	83.0	76.0	81.7	25.8	57.2
Mean	Resting			92.4 (13.6)	84.3 (12.5)	91.0 (13.3)	36.0 (9.8)	71.1 (14.5)
4	Hypoventilation	31	M	109.9	97.3	108.4	41.6	81.8
5	Hypoventilation	35	M	118.4	101.2	115.3	42.0	83.2

The mean and standard deviation of the resting values are also shown.

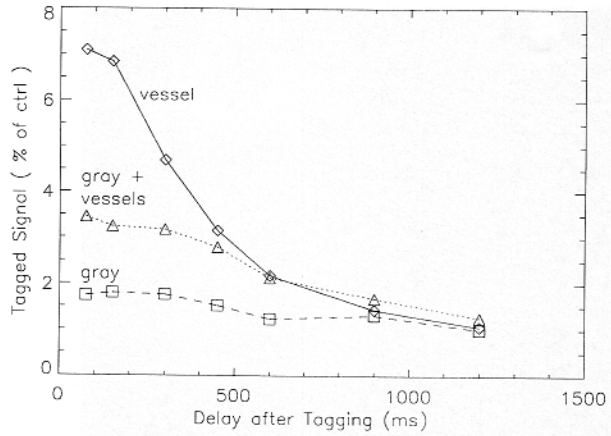

FIG. 4. Mean signal intensities in three types of gray matter regions, averaged across four subjects. Signal from regions containing only bright vessels on early delay images decays rapidly with delay. Signal from gray matter regions, which include some smaller bright vessels, decays more slowly. Finally, signal from gray matter regions selected for the absence of bright vascular structures remains virtually constant with delay. All three regions have similar signals at long delay times.

image with no contrast between gray and white matter, suggesting that the error was not related to perfusion. The basis for this difference, which varied from subject to subject, is uncertain; however, the amplitude never exceeded 20% of the gray matter perfusion signal in any subject.

Quantitative perfusion values for five of the subjects are shown in Table 1. We assumed a tissue transit time, δ, of 1,500 ms, a T_1 for blood of 1,100 ms (Bryant et al., 1990), and a brain–blood partition coefficient of 0.98 for gray matter and 0.82 for white matter (Herscovitch and Raichle, 1985). Mean gray matter flow was found to be 91, mean white matter flow was 36, and average flow was 71 ml 100 g^{-1} min^{-1}. Representative images calculated for one subject are shown in Fig. 5. Voluntary hypoventilation in two subjects caused a 40% increase in perfusion relative to rest (Fig. 6).

DISCUSSION

These results demonstrate the feasibility of obtaining high resolution, quantitative perfusion images of the human brain without exogenous tracers or arterial or venous blood sampling. Using the present technique, high quality perfusion images could be obtained from a single slice through the human brain in <5 min. Our results represent a major improvement in resolution relative to other techniques, except those obtained from the highest quality positron emission tomography (PET) studies. Since the resolution of the MR technique is limited only by the signal-to-noise ratio, further improvement in resolution should be obtainable with optimization of acquisition parameters, increased imaging time, more sensitive RF receiving coils, and higher field strength magnets.

Sensitivity of the perfusion images, motion insensitivity of results, and flexibility of scan timing were all enhanced by the use of echoplanar imaging. Interleaved subtraction essentially eliminated the need for subject constraint as proven by the perfusion images obtained in seven subjects that had no indication of motion artifact. Echoplanar imaging also improved the speed with which T_1 maps could be obtained. While echoplanar imaging is probably not essential for this technique—since interleaved acquisition and delay are compatible with standard spin warp spin and gradient echo sequences—echoplanar perfusion images will serve as a benchmark of motion insensitivity and image quality against which other acquisition methods must be compared.

Acquisition of images using different posttagging delays made it possible to estimate, δa, the arterial blood transit time. Measurement of the true tissue transit time is difficult and may be beyond the capabilities of MR techniques. Measurements of arterial transit time using other techniques are rare in the literature and subject to similar inaccuracies (Nagata and Asano, 1990). Introduction of a posttagging delay also eliminated the intense signal from large vessels, which, clearly, do not reflect tissue perfusion. This effect is a by-product of choosing w longer than δa. Bipolar gradient pulses may still be used but are unnecessary unless δa is longer than w. The presence of bright vessels in perfusion images acquired without bipolar gradients is an indication that a longer delay is necessary to achieve transit time insensitivity.

Perfusion images acquired with opposite signs of tagging gradient demonstrated small differences representing subtraction error. It has been suggested that the magnetization transfer spectrum may be asymmetric, resulting in subtraction errors when perfusion tagging is applied (Pekar et al., 1996; Stein et al., 1994). In our study, subtraction errors varied considerably from subject to subject, which argues against the existence of a fundamental asymmetry in the magnetization transfer spectrum. These small differences may simply be caused by slight offsets in the magnetic field due to variations in subject geometry, eddy currents, or other instrumental imperfections. Averaging the perfusion images obtained with opposite gradient sign dramatically decreases sensitivity to such errors, resulting in improved quantification.

An adequate quantification method for our images must take into account the presence of a considerable volume of tagged water in small arterial vessels, in addition to that in the tissue itself. Results of varying w suggest that the transit time to visible arterial structures is on the order of 200 ms while the transit time to the smaller vessels, which feed white matter and smaller gray matter structures, is on the order of 600 ms. Even

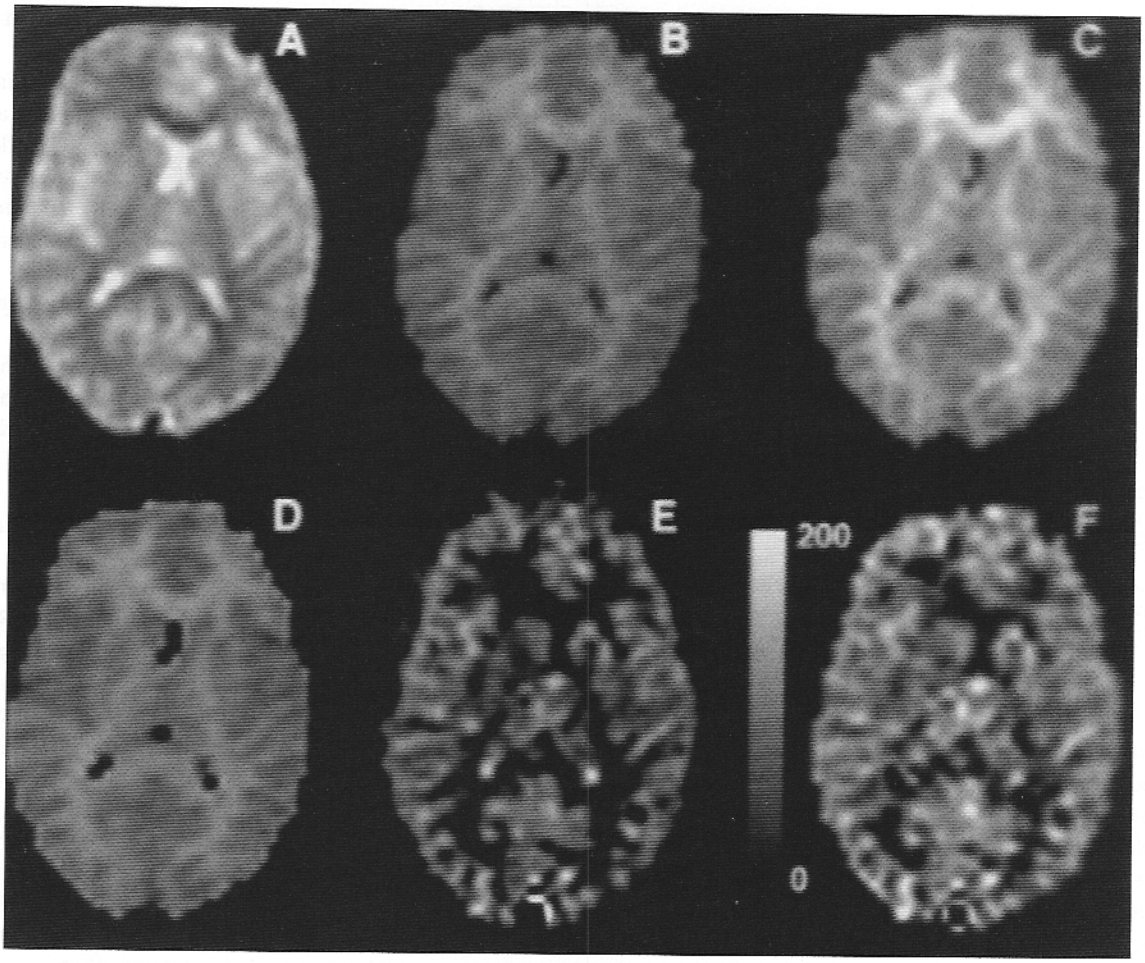

FIG. 5. Calculated images from a representative subject. Echoplanar images **(A)** are used to calculate images of $1/T_{1ns}$ **(B)** and $1/T_{1s}$ **(C),** so a perfusion calibration constant image **(D),** can be determined. Averaged difference images (control – inversion) **(E)** are then converted to quantitative perfusion images, **(F).** The quantitative perfusion image, in units of ml/100 g^{-1}/m^{-1}, was calculated assuming an average blood–brain partition coefficient of 0.9 (Herscovitch and Raichle, 1985).

when a 900-ms delay is employed, it is unlikely that all of the tagged blood reaches the tissue. Although this blood signal could be eliminated by increasing the delay time, at the cost of sensitivity, theoretical estimates indicate that the signal in the small vessels compromises neither resolution nor quantification. Image signal intensity for our experimental parameters is plotted as a function of tissue transit time in Fig. 7, assuming a δa of 600 ms. Although the image intensity is sensitive to tissue transit time, the dependence is very weak in gray matter and fairly weak in white matter. As the tissue transit time exceeds the tissue T_1, transit time sensitivity disappears because most of the signal is actually within the vascular compartment. Although we have selected a 900-ms delay for our studies of normal volunteers, a longer delay may be necessary to ensure transit time insensitivity in patients suffering from vascular disease, who frequently have longer arterial transit times.

Accurate quantification of perfusion requires knowledge of longitudinal tissue relaxation. The effects of magnetization transfer, due to the tagging pulse, must be considered in the measurement of T_1. We have measured T_1 of tissue both in the presence and absence of the tagging pulse. T_1 is measurably shorter during the tagging, and the fractional change in T_1 is roughly equal to the fractional change in signal intensity caused by magnetization transfer.

Zhang et al. (1992, 1995), have reported detailed theoretical and experimental studies of the relationship between T1, magnetization transfer, and perfusion quantification that support this relationship. Their work assumes that the macromolecular spins are fully saturated during tagging while the free spins are unaffected except by transfer. If this full saturation of macromolecular spins were accomplished, however, the observed signal intensity would be independent of tagging amplitude (Grad and Bryant, 1990). This situation is almost never observed in vivo since sufficiently high saturation power is rarely used. A more appropriate assumption would be that the exchange between the two or more water com-

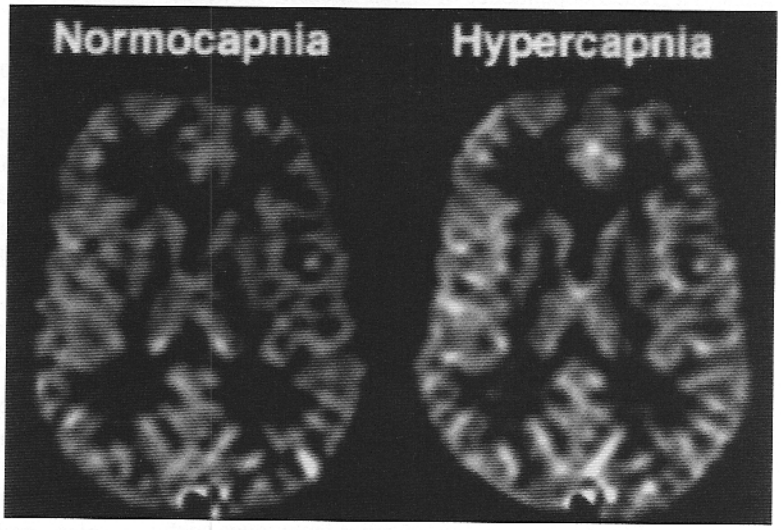

FIG. 6. Difference images (control – arterial spin tagging) from a subject during rest (left) and during voluntary hypoventilation (right). Cerebral perfusion increased by 34% during the hypercapnia induced by the hypoventilation.

partments is very fast compared to that of T_1. Under this assumption, the relative concentration of spins in all compartments remains unchanged when saturated (Caines et al., 1991). The relationship between T_1 change and signal saturation derived by Zhang et al. (1992) remains true under this new assumption. Both assumptions can be avoided if T_{1s} and T_{1ns} are measured directly, as in this study. Except for short transient effects, the longitudinal relaxation of tissues can be well characterized by these two time constants (Adler and Yeung, 1993; Yeung and Swanson, 1992). During the fitting of the T_1 decay curves, an accurate measure of magnetization transfer is also obtained. Since magnetization transfer is much greater in tissue than in CSF, the measured magnetization transfer could be used to estimate the amount of tissue in each voxel. Using this approach, gray matter perfusion values could be corrected for partial volume effects, which are particularly severe when atrophy is present.

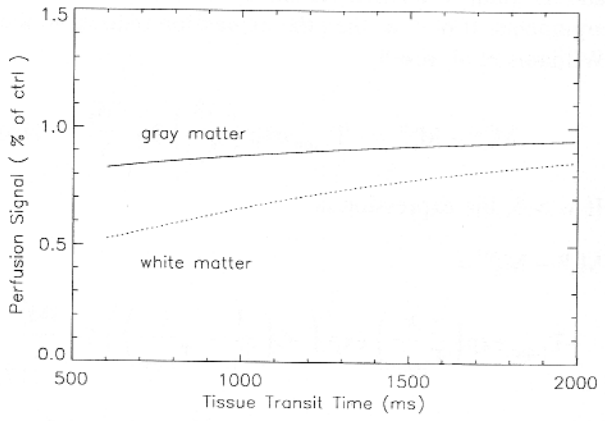

FIG. 7. Calculated signal in gray and white matter as a function of δ for blood flow of 60 ml g^{-1} m^{-1}, δa of 600 ms, w of 900 ms, and T_{1s} for gray and white matter as measured in the text. The calculation includes the effects of magnetization transfer and intraluminal spins. Results are largely independent of δ, suggesting that an accurate measure of δ is not necessary.

Quantitative perfusion values obtained with our method were in agreement with those measured by other techniques. Gray matter perfusion values of 91 ± 13 ml 100 g^{-1} min^{-1} and white matter values of 36 ± 10 ml 100 g^{-1} min^{-1} are slightly higher than PET measurements of resting perfusion (Lammertsma et al., 1990; Matthew et al., 1993; Quarles et al., 1993). Several factors may contribute to this difference. First, our volunteers were relatively young. CBF has been shown to be higher than average in young adults (Pantano et al., 1984) and in women (Gur et al., 1982, 1994). Excluding the two younger female subjects would have shifted the mean CBF values more towards literature values. Finally, the comparatively high resolution of our method as compared to that of PET may have more correctly separated gray from white matter, resulting in higher gray matter flows. Although arterial or end-tidal CO_2 levels were not measured, voluntary hypoventilation produced easily detectable changes in measured perfusion, consistent with the expected effects of hypercapnia on CBF. Literature values for CO_2 reactivity (Levine et al., 1991), 5% / mm Hg, suggests an increased P_aCO_2 of 8 mm Hg would achieve the observed 40% increase in flow.

Our theoretical model indicates that the fortuitously similar T_{1s} of blood and gray matter make quantification of gray matter flow virtually independent of transit time to the tissue, δ, when a sufficiently long tagging delay is employed (Fig. 2**A**). Images are perfectly independent of transit time to the vascular compartment, δa, for both gray and white matter as long as the transit time is shorter than the delay time. The need to account for transit time represented one of the major obstacles to quantification of perfusion, particularly in humans where the transit time is comparable to T_1. The shorter T_1 of white matter

leads to a greater dependence of signal intensity on tissue transit time (Fig. **2B**); however, this dependence is still markedly weaker than the exponential dependence of signal on transit time when no tagging delay is employed. When perfusion values are calculated assuming δ of 750 instead of 1,500 ms, white matter perfusion increases 32% but gray matter perfusion increases by only 8%. The remaining sensitivity of white matter flow to transit time still requires that a fairly accurate transit time value be used for accurate flow quantification.

The availability of a high resolution, quantitative cerebral perfusion imaging method requiring no injections, no arterial or venous sampling, and no ionizing radiation should contribute to a better understanding of cerebrovascular physiology and improve the diagnosis and treatment of stroke, trauma, neoplasms, seizures, degenerative disease, and other cerebral disorders. It is also readily combined with a variety of other techniques such as angiography, spectroscopy, or blood oxygenation-sensitive brain activation imaging. Adaptation of this technique to other body organs should also be possible with clear applications to a variety of circulatory disorders.

Acknowledgment: This work was supported in part by a grant from the National Institutes of Health, NS01668 (J.A.D.). The authors acknowledge helpful discussions with Drs. Rahim Rizi, David Roberts, Joseph McGowan, Ruben Gur, Abass Alavi, and Martin Reivich.

APPENDIX

The theory of spin tagging experiments is based on the modified Bloch equation (Detre et al., 1992),

$$\frac{dM_b}{dt} = \frac{M_b^0 - M_b}{T_{1b}} + fM_a - \frac{f}{\lambda}M_b = \frac{M_b^0 - M_b}{T_{1app}} + f\left(M_a - \frac{M_b^0}{\lambda}\right) \quad (11)$$

where f is the blood flow in ml/gm/s, λ is the brain-blood partition coefficient defined as the ml of water per gram tissue/ml water per ml blood, T_{1b} is the T_1 of brain tissue, M_b is the brain tissue magnetization, M_b^0 is the equilibrium brain tissue magnetization, M_a is the arterial blood magnetization, and T_{1app} is given by Eq. 2. Since all of the methods for quantifying blood flow rely on subtracting two images acquired with different arterial spin tagging but identical flow, we can simplify the Bloch equation to

$$\frac{d(M_b^{tag} - M_b^{ctrl})}{dt} + \frac{(M_b^{tag} - M_b^{ctrl})}{T_{1app}} = f(M_a^{tag} - M_a^{ctrl}) \quad (12)$$

The observed signal intensity difference can then be derived by direct integration once the arterial spins are defined.

Continuous inversion methods

First, we consider the continuous labeling experiment where spins are steadily inverted or saturated at a particular point in the arterial tree. We will also introduce a delay of duration, w, between the end of tagging and the acquisition of the image. At times before w, the tagged arterial blood at the tagging plane is given by

$$M_a^{tag} - M_a^{ctrl} = (1 - 2\alpha)\frac{M_b^0}{\lambda} - \frac{M_b^0}{\lambda} = -2\alpha\frac{M_b^0}{\lambda} \quad (13)$$

where we have employed Eq. 2 of Williams et al. (1992) and defined the inversion efficiency, α, which is one for inversion and one half for saturation. Because there is a delay between the tagging of the blood at the tagging plane and its arrival at the tissue, namely the transit time, δ, we must include the T_1 decay that occurs during that time, i.e.,

$$M_a^{tag} - M_a^{ctrl} = -2\alpha\frac{M_b^0}{\lambda}\exp\left(\frac{-\delta}{T_{1a}}\right) \quad (14)$$

Untagged blood begins to arrive at the slice before imaging only if $w > \delta$. The signal difference is given by

$$M_b^{tag} - M_b^{ctrl} = -\exp\left(\frac{-\delta}{T_{1a}}\right) 2\alpha\frac{fM_b^0}{\lambda}\int_{-\infty}^{\min[(\delta - w), 0]} dt \exp\left(\frac{t}{T_{1app}}\right) = -T_{1app}\exp\left(\frac{\min((\delta - w), 0)}{T_{1app}}\right)\exp\left(\frac{-\delta}{T_{1a}}\right) 2\alpha\frac{fM_b^0}{\lambda} \quad (15)$$

where we define $t = 0$ as the time the image is acquired and the min( ) function returns the minimum of its two arguments. If $\delta \geq w$, then the expression reduces to the Williams et al. result

$$M_b^{tag} - M_b^{ctrl} = -T_{1app}\exp\left(\frac{-\delta}{T_{1a}}\right) 2\alpha\frac{fM_b^0}{\lambda} \quad (16)$$

If $w > \delta$, the expression is

$$M_b^{tag} - M_b^{ctrl} = -T_{1app}\exp\left(\frac{-w}{T_{1app}}\right)\exp\left(-\delta\left(\frac{1}{T_{1a}} - \frac{1}{T_{1app}}\right)\right) 2\alpha\frac{fM_b^0}{\lambda} \quad (17)$$

Next, we consider the effect of magnetization transfer on the continuous labeling experiment with posttagging delay. Because T_{1app} is equal to T_{1s} during the tagging pulse and to T_{1ns} afterwards, the tissue magnetization must be calculated in two steps. Until w before the im-

aging, the off-resonance pulse is applied and T_{1s} must be used. The perfusion-related magnetization at that time is identical to the 0 delay experiment with T_{1s} inserted for T_{1app}

$$(M_b^{tag} - M_b^{ctrl}) = \frac{-2\, M_b^0\, f\alpha T_{1s}}{\lambda} \exp(-\delta/T_{1a}) \qquad (18)$$

At $t = -w$, the tissue signal becomes governed by the unsaturated equation where T_{1app} equals T_{1ns}. Substituting the above expression for the magnetization at $t = -w$ and integrating the modified Bloch equation from $-w$ to 0, the imaging time, yields

$$(M_b^{tag} - M_b^{ctrl}) = \frac{-2\, M_b^0\, f\alpha T_{1ns}}{\lambda} \exp(-\delta t/T_{1a})$$

$$\left[\exp[\min(\delta - w,0]/T_{1ns}) - \exp(-w/T_{1ns}) \left(1 - \frac{T_{1s}}{T_{1ns}}\right) \right] \qquad (19)$$

The arterial blood signal is also governed by a modified Bloch equation with one important distinction from the tissue equation. The probability of tissue water exiting through the veins is independent of when the water entered the tissue since diffusion and other properties rapidly mix the molecules. In contrast, the probability of arterial water exiting the vascular compartment is strongly determined by the time it entered. This necessitates a change to the outflow expression. The outflowing spins from the arterial vasculature compartment enter the tissue compartment so the outflow expression for the vascular compartment equals the expression for the inflow to the tissue, Eq. 14. The inflow is given by the same expression with δa substituted for δ. The vascular signal is then

$$(M_V^{tag} - M_V^{ctrl}) = \frac{-2\,\alpha\, M_b^0\, f}{\lambda} \left(\int_{-\infty}^{\min(\delta a - w,0)} dt \exp((t - \delta a)/T_{1a}) - \int_{-\infty}^{\min(\delta - w,0)} dt \exp((t - \delta)/T_{1a}) \right) = \frac{-2\,\alpha\, M_b^0\, f}{\lambda} (\exp[(\min(\delta a - w, 0) - \delta a)/T_{1a})] - \exp((\min(\delta - w, 0) - \delta)/T_{1a})) \qquad (20)$$

The observed signal is given by the sum of the tissue and arterial signals.

In reality, blood tagged in the carotid and vertebral arteries does not all travel at the same velocity and, consequently, a spread of transit times to the vascular compartment and tissue are required to describe the dynamics of blood. Magnetization can be calculated in this more general case by replacing the flow, f, in the expression for observed signal with an expression $f(\delta, \delta a)$ that represents the fraction of blood flow that experiences the specified transit times. The integral of this function over all transit times must equal the total flow, while the integral of the observed signal over all transit times gives the total signal. Since the signal change can be made insensitive to transit time, this added level of complexity may be unnecessary.

Pulsed inversion

A preliminary model for the signal observed in pulsed inversion experiments (Buxton et al., 1995) has highlighted the role of the temporal spread of the arriving bolus and utilized data from multiple inversion times to quantify the relative perfusion change during an activation. Following Buxton et al., we will assume a square bolus of duration τ that begins to arrive at the tissue following a delay, δ, caused by arterial transit times. Their method also assumes that the duration of the bolus is due entirely to the geometric spread of the tagging slab, i.e., there is no dispersion of transit times from the end of the slab to the tissue. Although this is a questionable assumption, we will employ it below. If the quantification depends heavily on either δ or τ, it will be highly suspect. All of the tagged arterial spins are inverted simultaneously at time $-TI$. For times between $-TI + \delta$ and $-TI + \tau$, inflowing spins are given by

$$M_a^{tag} - M_a^{ctrl} = -2\,\alpha \frac{M_b^0}{\lambda} \exp\left(\frac{-(t + TI)}{T_{1a}}\right) \qquad (21)$$

The signal difference at the imaging time, $t = 0$, is given by

$$M_b^{tag} - M_b^{ctrl} = -\exp\left(\frac{-TI}{T_{1a}}\right) 2\,\alpha \frac{f\, M_b^0}{\lambda} \int_{\delta - TI}^{\min(0,\ \delta + \tau - TI)} dt \exp\left(t\left(\frac{1}{T_{1app}} - \frac{1}{T_{1a}}\right)\right) = -\exp\left(\frac{-TI}{T_{1app}}\right) 2\,\alpha \frac{f\, M_b^0}{\lambda} \frac{\left[\exp\left(\min(TI, \delta + \tau)\left(\frac{1}{T_{1app}} - \frac{1}{T_{1a}}\right)\right) - \exp\left(\delta\left(\frac{1}{T_{1app}} - \frac{1}{T_{1a}}\right)\right)\right]}{\left(\frac{1}{T_{1app}} - \frac{1}{T_{1a}}\right)} \qquad (22)$$

If the bolus duration, τ, is sufficiently long that the full bolus has not entered the slice by the imaging time, then this simplifies to

$$M_b^{tag} - M_b^{ctrl} = -\exp\left(\frac{-TI}{T_{1app}}\right) 2\,\alpha \frac{f\, M_b^0}{\lambda} \qquad (23)$$

$$\frac{\left[\exp\left(\mathrm{TI}\left(\frac{1}{T_{1app}}-\frac{1}{T_{1a}}\right)\right)-\exp\left(\delta\left(\frac{1}{T_{1app}}-\frac{1}{T_{1a}}\right)\right)\right]}{\left(\frac{1}{T_{1app}}-\frac{1}{T_{1a}}\right)}$$

while if the entire bolus has entered the tissue, then

$$M_b^{tag}-M_b^{ctrl}=-\exp\left(\frac{-TI}{T_{1app}}\right)2\,\alpha\,\frac{f\,M_b^0}{\lambda}\frac{\left[\exp\left((\delta+\tau)\left(\frac{1}{T_{1app}}-\frac{1}{T_{1a}}\right)\right)-\exp\left(\delta\left(\frac{1}{T_{1app}}-\frac{1}{T_{1a}}\right)\right)\right]}{\left(\frac{1}{T_{1app}}-\frac{1}{T_{1a}}\right)} \quad (24)$$

If T_{1app} is comparable to T_{1a}, this reduces to

$$M_b^{tag}-M_b^{ctrl}=-\exp\left(\frac{-TI}{T_{1app}}\right)2\,\alpha\,\frac{f\,M_b^0}{\lambda}\,\tau \quad (25)$$

The duration of the bolus, τ, is given by the volume of the tagged arteries, V_a, divided by the total CBF, F. Consequently, the signal intensity becomes dependent on the arterial blood volume and the ratio of the flow to the total CBF, instead of the absolute blood flow.

$$M_b^{tag}-M_b^{ctrl}=-\exp\left(\frac{-TI}{T_{1app}}\right)2\,\alpha\,\frac{f\,M_b^0}{F\,\lambda}\,V_a \quad (26)$$

It is essential to ensure that TI is shorter than τ in order to obtain quantitative, absolute perfusion images. If TI is shorter than τ, larger arteries should also contain tagged blood and they will be apparent in the images. The lack of bright vessels in the perfusion images of previous studies (Edelman et al., 1994; Kim, 1995; Kwong et al., 1995) suggest that τ was too short to quantify absolute perfusion.

REFERENCES

Adler RS, Yeung HN (1993) Transient decay of longitudinal magnetization in heterogeneous spin systems under selective saturation. III. Solution by projection operators. *J Magn Reson A* 104:321–330

Belliveau JW, Rosen BR, Kantor HL, Rzedzian RR, Kennedy DN, McKinstry RC, Vevea JM, Cohen MS, Pykett IL, Brady TJ (1990) Functional cerebral imaging by susceptibility contrast. *Magn Reson Med* 14:538–546

Bottomley PA, Foster TH, Argersinger RE, Pfeifer LM (1984) A review of normal tissue hydrogen NMR relaxation times and relaxation mechanisms from 1–100 MHz: Dependence on tissue type, NMR frequency, temperature, species, excision and age. *Med Phys* 11:425–448

Bryant RG, Marill K, Blackmore C, Francis C (1990) Magnetic relaxation in blood and blood clots. *Magn Reson Med* 13:133–144

Buxton RB, Frank LR, Siewert B, Warach S, Edelman RR (1995) A quantitative model for EPISTAR perfusion imaging. In: *Society of Magnetic Resonance, Third Meeting,* Berkeley, Society of Magnetic Resonance, 132

Caines GH, Schleich T, Rydzewski JM (1991) Incorporation of magnetization transfer into the formalism for rotating-frame spin-lattice proton NMR relaxation in the presence of an off-resonance-irradiation field. *J Magn Reson* 95:558–566

Detre JA, Leigh JS, Williams DS, Koretsky AP (1992) Perfusion imaging. *Magn Reson Med* 23:37–45

Dixon WT, Du LN, Faul DD, Gado M, Rossnick S (1986) Projection angiograms of blood labeled by adiabatic fast passage. *Magn Reson Med* 3:454–462

Edelman RR, Siewert B, Darby DG, Thangaraj V, Nobre AC, Mesulam MM, Warach S (1994) Qualitative mapping of cerebral blood flow and functional localization with echo-planar MR imaging and signal targeting with alternating radio frequency. *Radiology* 192:513–520

Grad J, Bryant RG (1990) Nuclear magnetic cross-relaxation spectroscopy. *J Magn Reson* 90:1–8

Gur RC, Gur RE, Orbrist WD, Hungerbuhler JP, Younkin D, Rosen AD, Skolnick BE, Reivich M (1982) Sex and handedness differences in cerebral blood flow during rest and cognitive activity. *Science* 217:659–661

Gur RC, Ragland JD, Resnick SM, Skolnick BE, Jaggi J, Muenz L, Gur RE (1994) Lateralized increases in cerebral blood flow during performance of verbal and spatial tasks: relationship with performance level. *Brain and Cog* 24:244–258

Henkelman RM, Neil JJ, Xiang QS (1994) A quantitative interpretation of IVIM measurements of vascular perfusion in the rat brain. *Magn Reson Med* 32:464–469

Herscovitch P, Raichle ME (1985) What is the correct value for the brain-blood partition coefficient for water. *J Cereb Blood Flow Metab* 5:65–69

Kim SG (1995) Quantification of relative cerebral blood flow change by flow-sensitive alternating inversion recovery (FAIR) technique: application to functional mapping. *Magn Reson Med* 34:293–301

Kwong KK, Belliveau JW, Chesler DA, Goldberg IE, Weisskoff RM, Poncelet BP, Kennedy DN, Hoppel BE, Cohen MS, Turner R, Cheng HM, Brady TJ, Rosen BR (1992) Dynamic magnetic resonance imaging of human brain activity during primary sensory stimulation. *Proc Natl Acad Sci USA* 89:5,675–5,679

Kwong KK, Chesler DA, Weisskoff RM, Donahue MD, Davis TL, Ostergaard L, Campbell TA, Rosen BR (1995) MR perfusion studies with T1-weighted echo planar imaging. *Magn Reson Med* 34: 878–887

Lammertsma AA, Cunningham VJ, Deiber MP, Heather JD, Bloomfield PM, Nutt J, Frackowiak RSJ, Jones T (1990) Combination of dynamic and integral methods for generating reproducible functional CBF images. *J Cereb Blood Flow Metab* 10:675–686

Larsson HBW, Frederiksen J, Kjaer L, Henriksen O, Olesen J (1988) In vivo determination of T1 and T2 in the brain of patients with severe but stable multiple sclerosis. *Magn Reson Med* 7:43–55

Levine RL, Dobkin JA, Rozental JM, Satter MR, Nickles RJ (1991) Blood flow reactivity to hypercapnia in strictly unilateral carotid disease: preliminary results. *J Neurol Neurosurg Psychiatry* 54: 204–209

Matthew E, Andreason P, Carlson RE, Herscovitch P, Pettigrew K, Cohen R, King C, Johanson CE, Paul SM (1993) Reproducibility of resting cerebral blood flow measurements with H215O positron emission tomography in humans. *J Cereb Blood Flow Metab* 13: 748–754

Morrison C, Henkelman RM (1995) A model for magnetization transfer in tissues. *Magn Reson Med* 33:475–482

Nagata K, Asano T (1990) Functional image of dynamic computed tomography for the evaluation of cerebral hemodynamics. *Stroke* 21:882–889

Pantano P, Baron J, Lebrun-Grandie P, Duquesnoy N, Bousser M, Comar D (1984) Regional cerebral blood flow and oxygen consumption in human aging. *Stroke* 15:635–41

Pekar J, Jezzard P, Roberts DA, Leigh JS, Frank JA, McLaughlin AC (1996) Perfusion imaging with compensation for asymmetric magnetization transfer effects. *Magn Reson Med* 35:70–79

Quarles RP, Mintun MA, Larson KB, Markham J, MacLeod AM, Raichle ME (1993) Measurement of regional cerebral blood flow

with positron emission tomography: a comparison of [^{15}O]water to [^{11}C]butanol with distributed-parameter and compartmental models. *J Cereb Blood Flow Metab* 13:733–747

Roberts DA, Detre JA, Bolinger L, Insko EK, Leigh JS (1994) Quantitative magnetic resonance imaging of human brain perfusion at 1.5 T using steady-state inversion of arterial water. *Proc Natl Acad Sci USA* 91:33–37

Silva AC, Zhang W, Williams DS, Koretsky AP (1995) Multi-slice MRI of rat brain perfusion during amphetamine stimulation using arterial spin labeling. *Magn Reson Med* 33:209–214

Steen RG, Gronemeyer SA, Kingsley PB, Reddick WE, Langston JS, Taylor JS (1994) Precise and accurate measurement of proton T1 in human brain in vivo: validation and preliminary clinical application. *J Magn Reson Imaging* 4:681–691

Stein AD, Roberts DA, McGowan J, Reddy R, Leigh JS (1994) Asymmetric cancellation of magnetization transfer effects. In: *Proceedings of the Society of Magnetic Resonance Second Meeting,* Berkeley, Society of Magnetic Resonance, 880

Weisskoff RM, Chesler D, Boxerman JL, Rosen BR (1993) Pitfalls in MR measurement of tissue blood flow with intravascular tracers: which mean transit time? *Magn Reson Med* 29:553–558

Williams DS, Detre JA, Leigh JS, Koretsky AP (1992) Magnetic resonance imaging of perfusion using spin inversion of arterial water. *Proc Natl Acad Sci USA* 89:212–216

Williams DS, Detre JA, Zhang W, Koretsky AP (1993) Fast serial MRI of perfusion in the rat brain using spin inversion of arterial water. *Bull Magn Reson* 15:60–63

Yeung HN, Swanson SD (1992) Transient decay of longitudinal magnetization in heterogeneous spin systems under selective saturation. *J Magn Reson* 99:466–479

Zhang W, Silva AC, Williams DS, Koretsky AP (1995) NMR measurement of perfusion using arterial spin labeling without saturation of macromolecular spins. *Magn Reson Med* 33:370–376

Zhang W, Williams DS, Detre JA, Koretsky AP (1992) Measurement of brain perfusion by volume-localized NMR spectroscopy using inversion of arterial water spins: accounting for transit time and cross-relaxation. *Magn Reson Med* 25:362–371